# Formation of Highly Condensed Ferric Stearate Monolayers at the Air−Water Interface

**A. Datta* and M. K. Sanyal**

*Surface Physics Division, Saha Institute of Nuclear Physics, 1/AF Bidhannagar, Calcutta 700 064, India*

**A. Dhanabalan and S. S. Major**

*Physics Department, Indian Institute of Technology, Powai, Mumbai 400 076, India*

*Received: May 22, 1997*[⊗]

Pressure−molecular area isotherms of a Langmuir monolayer of preformed ferric stearate on water have been studied at various temperatures, compression rates, and pH values. The isotherms indicate anomalously small areas per molecule for the ferric stearate monolayers. A probable model is put forward to explain the small molecular areas. This model retains the area per hydrocarbon chain to 18 Å observed in other similar systems, with a head-to-tail ratio of 1:3, but assigns a dominant role to hydrophobic forces in forming and stabilizing the monolayer. The X-ray reflectivity profile calculated from this model matches well with the measured data of deposited Langmuir−Blodgett film of ferric stearate.

## 1. Introduction

Langmuir monolayers are formed at the interface of two liquids or at an air−liquid interface, the most common being the air−water interface. They are formed by molecules (amphiphiles) that have a hydrophilic (polar) and a hydrophobic (nonpolar) part, the head and the tail parts, respectively.[1] When the amphiphiles from a Langmuir monolayer are transferred onto a suitable solid substrate, repeated transfer is possible. This leads to a multilayer of alternate heads and tails, known as a Langmuir−Blodgett (LB) film.[2] A very interesting aspect of Langmuir monolayers is the richness of the phases they exhibit, depending on external conditions such as surface pressure, temperature, and pH of the aqueous substrate.[3] Fatty acids with long hydrcarbon tails are studied very frequently as they have a very simple structure with only one tail per head and also because most of the members in their homologous series easily form Langmuir monolayers and LB films. The surface pressure ($\pi$) vs specific molecular area (A) isotherms of monolayers of fatty acids have been studied thoroughly for these phases, and the structures of the phases have been determined, mostly from grazing incidence X-ray scattering studies. From these studies it is known that the phases are two-dimensional lattices differing from one another in lattice constants, tilt angles and tilt azimuth of the tails, the hydrocarbon backbone−plane ordering, and the positional and orientational correlation lengths.[4−12] In all these monolayers the head is found to be immersed in the water subphase while the tail part sticks out, though the exact location of the head relative to the water surface has not been determined. This configuration is also expected energetically if the attractive (hydrophilic) interaction between water and the head and the repulsive (hydrophobic) interaction between water and the tail both have some contribution in the overall interaction energy of the monolayer. In comparison, however, the picture for monolayers of fatty acid salts of metals is far from complete.[13−19] The composition of such monolayers and, in particular, the head-to-tail ratio have been clearly ascertained only for cadmium arachidate.[19] For that particular system the head-to-tail ratio is found to be 1:1, and the headgroups ($CdOH^+$ ions) form a lattice below the water surface which is a supercell of the lattice formed by the tails (arachidate ions). An important point to note in this context is that the standard procedure to form the monolayers of the fatty acid salts is not to spread a solution of the salt on water but to form the salt monolayer on the water surface through a reaction of a fatty acid monolayer with the metal ions dispersed in the water subphase. In this method the number of metal ions and the number of acid molecules available are far from equal. This introduces a large uncertainty in the composition of the monolayer. In case of fatty acid salts it is also known from both Langmuir monolayer data and X-ray[20−22] and atomic force microscopy[23−26] data on LB films that the head−head and head−tail interactions play a very important role in the nature of the monolayers as well as in the process of transfer. Data for fatty acid salts of metals with valency three or more are even more incomplete. Studies on ferric stearate and ferric arachidate, both three-tailed amphiphiles, have focused mainly on the aspects of deposition of the monolayers as Langmuir−Blodgett (LB) films and measuring the magnetic properties of these LB films.[27−30] In fact, for such monolayers even a careful measurement of the $\pi$−A isotherms have not been carried out. If a monolayer of a preformed ferric salt of a fatty acid is spread on water, the uncertainty in the monolayer composition is much reduced, and the information obtained from the isotherms would be close to that from a monolayer of three-tailed amphiphiles. We believe that the configurations of molecules in such a monolayer would be quite different from those of single-tailed amphiphiles, and a study of the isotherms would contribute to the understanding of the interactions responsible for formation and stability of such complex monolayers. In this communication we report results of isotherm studies of a Langmuir monolayer of preformed ferric stearate (FeSt) over the temperature range 20−30 °C and the isotherm of a stearic acid (StA) monolayer measured at 20 and 25 °C. Experiments were performed over pure water substrate and at pH ≃2.6−2.7 and at various compression (decompression) rates.

## 2. Experimental Details

**2.1. Sample Preparation and Purification.** Ferric stearate was prepared by adding measured amount ferric sulfate (E. Merck GmbH, 99%) solution to freshly prepared sodium stearate solution in hot, distilled water until the residual solution was slightly alkaline (pH ≃8.0). The sodium stearate itself was prepared from direct reaction of measured amounts of sodium hydroxide (E. Merck GmbH, 99%) and stearic acid (Sigma, 99%) in hot water. FeSt is completely insoluble in water at all

[⊗] Abstract published in *Advance ACS Abstracts,* October 1, 1997.

S1089-5647(97)01703-3 CCC: $14.00 

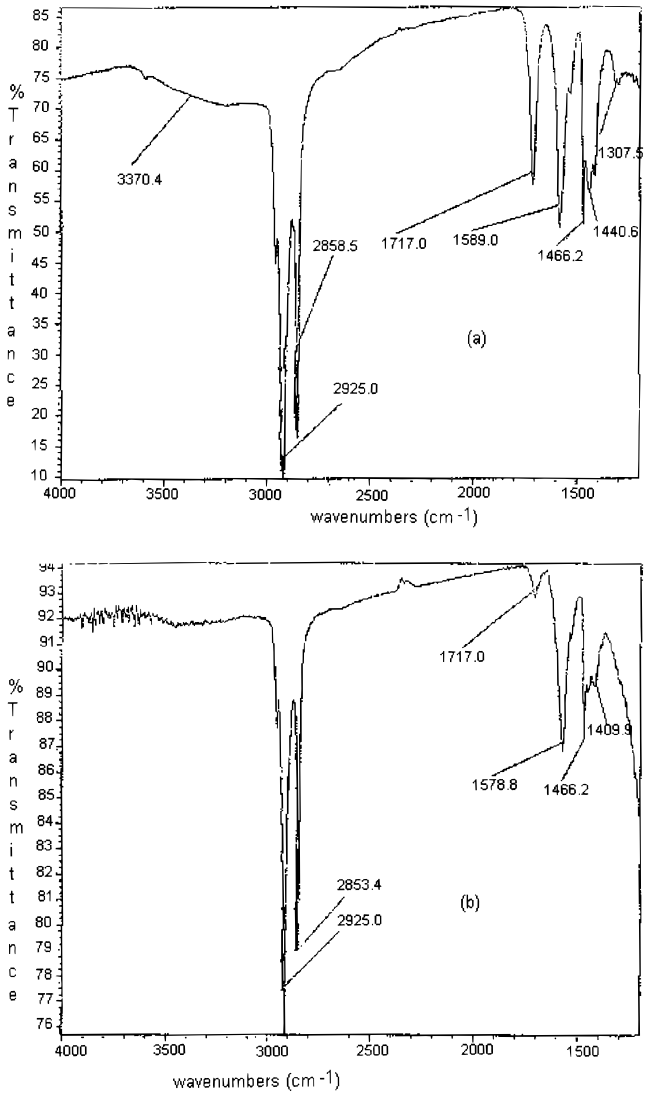


**Figure 1.** Fourier transform infrared spectra of (a) ferric stearate before final purification (FeSt1) and (b) after final purification (FeSt2).

temperatures and also in ethyl alcohol and acetone and was collected as a surfactant through filtration under reduced pressure. It was washed repeatedly with hot, double distilled water, acetone, and ethyl alcohol to remove unreacted StA, sodium stearate, and other organic and inorganic impurities. This procedure yielded a sample that we shall designate by FeSt1. FeSt1 was dissolved in chloroform by sonication and cast as a film on calcium fluoride (cleaned with chloroform and acetone). A Fourier transform infrared (FTIR) spectrum of this cast film was obtained. The FTIR spectrum of FeSt1 is presented in Figure 1a. It shows the carboxylate asymmetric stretch band (∼1580 $cm^{-1}$) and symmetric stretch band (∼1440 $cm^{-1}$) which indicate the presence of a fatty acid salt. The spectrum also shows a COOH deformation band (∼1300 $cm^{-1}$) and a carbonyl stretch band (∼1717 $cm^{-1}$), indications of unreacted fatty acids in the sample. The strong bands at ∼2850 and 2925 $cm^{-1}$ belonging to methylene and methyl symmetric stretch, respectively, and the methylene scissor vibration band (∼1466 $cm^{-1}$) are expected to appear in both fatty acids and fatty acid salts with a long hydrocarbon chain. No hydroxyl bands are visible in the FTIR spectrum, indicating the absence of any detectable quantity of hydroxy salts in FeSt1.[31] A portion of FeSt1 was first sonicated with petroleum ether and filtered. The residue was then sonicated with carbon tetrachloride, and the filtered residue was sonicated with *n*-hexane. The residue obtained by filtering this suspension will be named FeSt2. The FTIR spectrum of this sample was obtained in the same way as above and is shown in Figure 1b. The COOH deformation band is absent, and the carbonyl stretch band has become very weak whereas the carboxylate stretch bands do not show a large change in intensity. Again, as in FeSt1, hydroxyl bands are absent. As expected, the methylene and methyl symmetric stretch bands and the methylene scissor band are present with almost no change in strength. Thus, the sample consists of a long-chain fatty acid salt with no hydroxy salts and only a very small amount of unreacted fatty acid. Further purification efforts produced no change in the spectrum, and hence the sample FeSt2 was used as closest to pure FeSt in subsequent experiments.

**2.2. Monolayer Spreading and Measurements.** The samples FeSt1 and FeSt2 were dissolved in chloroform by sonication for ∼10 min to give a clear yellow solution in both cases. Concentrations of the solutions of FeSt1 and FeSt2 used in the experiments described below were 0.490 and 0.500 mg/mL, respectively. A solution in chloroform (0.528 mg/mL) was made of the StA sample from which the FeSt had been prepared. Monolayers of FeSt1, FeSt2, and StA were spread in a Langmuir trough (KSV 3000, Finland) with a temperature controller of stability better than ±0.3 °C and a compound calomel electrode for measurement of pH. The subphase used in most cases was Milli-Q deionized and ultrafiltered water with resistivity 18.2 MΩ cm and pH ∼ 5.55−5.65 (normal). The pH of the subphase was changed to ∼2.65−2.75 (low) by addition of 1 mL of 1 N hydrochloric acid to 1.3 L of this water. For isotherm measurements 150 $\mu$L of the samples was spread whereas for deposition of LB films 300 $\mu$L was used. Isotherm measurements for FeSt2 were carried out at 20, 25, and 30 °C, at normal and low pH, and at compression (decompression) rates of 0.3, 2.0, and 6.0 $Å^2$/(molecule min). For FeSt1, isotherms were measured at 20 and 25 °C and at the same compression rates but only at normal pH, while for StA the temperatures were 20 and 25 °C, and both pHs were used with only a 0.6 $Å^2$/(molecule min) compression rate. Each set of measurements started from a fully relaxed monolayer to reach the condensed phase and then decompressing it at the same rate back to full relaxation. This provided the compression−decompression isotherm (CDI). The monolayer was then recompressed at the same rate to collapse, and the collapse isotherm (COI) was measured. The trough and other accessories were cleaned thoroughly, and a new monolayer was spread before each such set.

**2.3. LB Film Deposition and Measurements.** An 11-monolayer Langmuir−Blodgett film of FeSt2 was deposited on calcium fluoride cleaned with chloroform and acetone. Calcium fluoride is a hydrophilic substrate. The deposition was Y-type, beginning with the substrate under water, and the dipping rate was 3 mm/min. The monolayer was compressed at the rate of 2.0 $Å^2$/(molecule min) to $\pi$ = 30 mN/m where the LB film was deposited. The temperature was 25 °C, and the pH was normal. The layer always came out dry from the water, but nevertheless a drying time of 15 min was allowed after each down−up cycle. A transfer ratio of ∼1.5−2.0 was obtained. The FTIR spectrum of this LB film showed almost identical bands as for bulk FeSt2 (Figure 1b). A nine-monolayer Langmuir−Blodgett film of FeSt2 was deposited on Si(100) substrate and cleaned (and hydrophilized) by first heating with $NH_3$:$H_2O_2$ = 1:1 (by volume) for 20 min, followed by washing with acetone and deionized water. Deposition conditions were the same as above except that the drying time was 10 min. The transfer ratio obtained was also in the same range. Grazing incidence X-ray reflectivity data of the LB film were collected using a rotating anode X-ray generator (FR 591, Enraf Nonius) at the Cu $K\alpha_1$ line (monochromatized by a Si(111) crystal face)

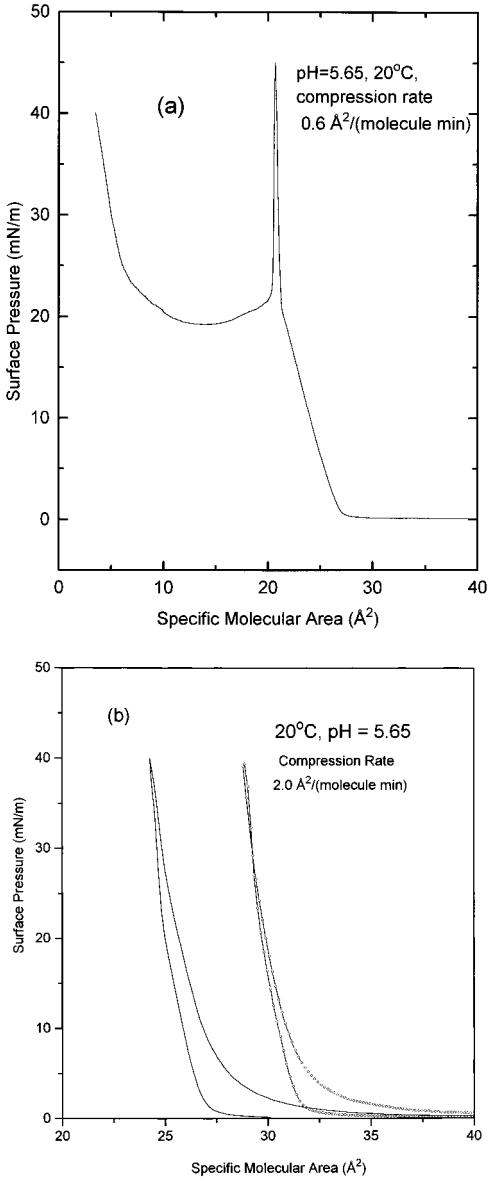


**Figure 2.** (a) Collapse isotherm of Langmuir monolayer of stearic acid. (b) Compression−decompression isotherms (below collapse pressure) of FeSt1 (line) and FeSt2 (line + circle) monolayers on water surface.

and a triple axis spectrometer (Optix Microcontrole). The step size in $q$ ($= (4\pi/\lambda) \sin\theta$, where $\theta$ is the angle of incidence and $\lambda$ is the X-ray wavelength) was 0.0007 Å$^{-1}$, and the instrumental resolution ($\delta q$) was 0.00018 Å$^{-1}$.

## 3. Monolayers: Specific Molecular Area

**3.1. Condensed Phase.** Molecular weights of 284.48 for StA and 905.0 for FeSt were used to calculate the area per molecule ($A$) in the respective monolayers. The collapse isotherm of stearic acid on water (pH = 5.65) at 20 °C and with the compression rate of 0.6 Å$^2$/(molecule min) is shown in Figure 2a. This curve, whose characteristics are well-known, has been used here mainly for calibrating the trough and for comparing with the isotherms of FeSt1 and FeSt2. The COI is seen to rise at the surface pressure ≃0.8 mN/m and a specific molecular area ≃26.9 Å$^2$. It makes a transition to the most condensed phase at $\pi \simeq 20.8$ mN/m and $A \simeq 21.2$ Å$^2$. These values are in good agreement with quoted values for the stearic acid monolayer on pure water at room temperatures,[32] underscoring the reliability of the $\pi-A$ measurements obtained from this trough. We turn now to a comparison of isotherms of FeSt1 and FeSt2. For this we choose the CDI's of these two samples with the same temperature and pH as for StA above but with the compression rate of 2.0 Å$^2$/(molecule min). These CDI's are shown in Figure 2b. The main effects of presence of unreacted stearic acid (in FeSt1) are (1) a shift of the whole CDI to lower specific molecular areas and (2) appearance of a small kink in the compression isotherm at $\pi \simeq 21.1$ mN/m and $A \simeq 25.6$ Å$^2$. The compression isotherm of FeSt2 rises from a small (∼0.1 mN/m) surface pressure with $A \simeq 40$ Å$^2$ to a condensed phase from $\pi \simeq 3.4$ mN/m and $A \simeq 32.9$ Å$^2$. After that the isotherm rises continuously to a specific molecular area of 28.8 Å$^2$ at 40 mN/m. On decompression the isotherm falls sharply to $\pi \simeq 23.45$ mN/m with $A \simeq 29.5$ Å$^2$ and from that point somewhat more slowly back to the low-pressure phase from $\pi \simeq 1.4$ mN/m with $A \simeq 31.7$ Å$^2$. For FeSt1 the condensed phase starts from $\pi \simeq 3.4$ mN/m and $A \simeq 29.8$ Å$^2$; at 40 mN m$^{-1}$ the specific molecular area is 24.3 Å$^2$, the decompression curve falls sharply to $\pi \simeq 22.7$ mN/m with $A \simeq 24.7$ Å$^2$, and the final transition to the low-pressure phase occurs at $\pi \simeq 1.4$ mN m$^{-1}$ with $A \simeq 27.1$ Å$^2$. The fact that the appearance of a "phase-transition kink" in the isotherm of FeSt1 monolayer is correlated with the presence of unreacted stearic acid has to be considered while examining the isotherms of FeSt2, as FTIR shows presence of small amount of stearic acid in the latter. However, the most striking result from the above figure is the anomalously small specific molecular area for either monolayer, and especially the purified FeSt2 monolayer, throughout the condensed phase. The anomaly becomes apparent if we consider that the FTIR spectral evidence shows the samples to be composed of ferric stearate molecules without any hydroxyl group, i.e., with three hydrocarbon chains per molecule, together with the known result that the smallest area per hydrocarbon chain in fatty acids and fatty acid salts is about 18 Å$^2$.[33,34] Isotherm data of StA rule out the possibility of calibration errors for the trough. Another important source of anomalous results is the loss of monolayer material to the subphase during compression. To test this, we have used a set of measurements comprising of a compression−decompression−recompression to collapse cycle, all at the same compression (decompression) rate of 0.3 Å$^2$/(molecule min), and at 25 °C and pH = 5.65. In Figure 3 we have shown the results of this measurement set. The compres-

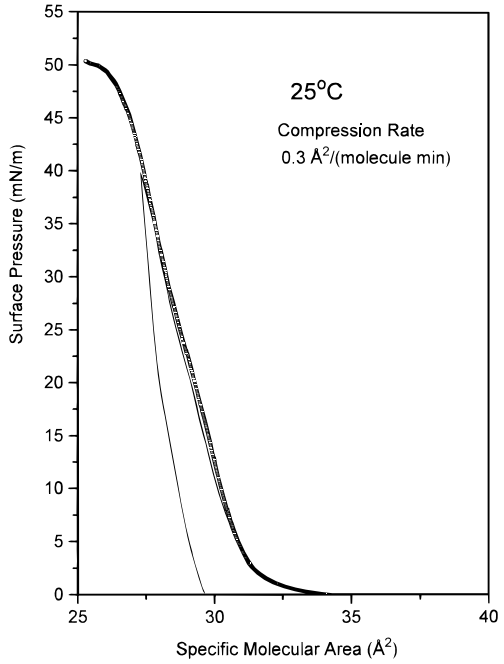


**Figure 3.** Single-cycle compression−decompression (line) and collapse (circle) isotherms of FeSt2 monolayer on water.

sion curve starts from a dilute phase, undergoes a transition to a condensed phase at $A = 31.30$ Å$^2$ ($\pi = 2.99$ mN/m), and attains $\pi = 40$ mN/m at $A = 27.3$ Å$^2$. From that point the decompression begins which relaxes the monolayer fully. The second compression ends in a collapse at $A = 26.10$ Å$^2$ and $\pi = 49.42$ mN/m. The close quantitative agreement between the compression and collapse curves eliminates the possibility of material loss. On the other hand, the specific molecular area of the monolayer in the most condensed phase (just before collapse), extrapolated to $\pi = 0$ is about 31.1 Å$^2$ showing that the anomaly in the specific molecular area is very much present even for such slow compression−decompression.

**3.2. Monolayer Decompression.** Decompression for ferric stearate (Figure 3) starts from $\pi = 40$ mN/m at $A = 27.3$ Å$^2$ with a steep fall in $\pi$ to ≃22.0 mN/m at $A = 27.9$ Å$^2$ and then falls more slowly, entering the dilute phase at $A = 29.5$ Å$^2$. The reproducibility of the initial condition of the monolayer, described in the previous section, precludes any material loss and hence, the sharp drop in surface pressure at almost constant specific molecular area is not due to collapse or nucleation of the monolayer at constant area. Rather this, along with the large area within the compression−decompression loop, indicates that the decompression processes are basically different from the processes occurring during compression of this monolayer.

## 4. Monolayers: Collapse Behavior

In Figure 2a we see the collapse isotherm of stearic acid. It undergoes a collapse at $\pi$≃45.1 mN/m and $A \simeq 20.6$ Å$^2$. The surface pressure falls sharply to ≃22.6 mN/m where the area per molecule is ≃20.4 Å$^2$, which corresponds to collapse at constant specific molecular area. After this the curve shows a plateau region up to A ≃ 7.4 Å$^2$ and then starts to rise again. This collapse behavior agrees with previous observations on StA at pH < 6 where the plateau has been interpreted as a monolayer to trilayer coexistence region.[35−37] It should be noted that the compression rate (0.6 Å$^2$/(molecule min) is an order of magnitude lower than the lowest compression rate for which crystallite formation on the water surface at constant surface pressure has been observed for stearic acid.[35] The nature of collapse in FeSt monolayers is distinct from that of StA. This is obvious from any COI of FeSt2, e.g. Figure 3, and comparison with Figure 2a, i.e., for similar pH values and compression rates. The collapse pressure in FeSt2 monolayers is higher (∼50−60 mN/m) than that of the StA monolayer (≃45.1 mN/m), indicating a more hydrophobic nature of the FeSt2 monolayer over pure water. More important, however, is the fact that instead of a sharp drop in the surface pressure at collapse as in the StA monolayer, the FeSt2 monolayer exhibits collapse at constant surface pressure even at the very low compression rate of 0.3 Å$^2$/(molecule min). Similar behavior has been observed in stearic acid at pH > 6[36] where it has been inferred that this high-pressure plateau corresponds to a first-order buckling transition.[38] This buckling is also observed in LB films of divalent salts[23−26] and has, in general, been related to the asymmetry in the areas occupied by head and tail groups.[38] For trivalent ferric stearate, this asymmetry is expected to be more enhanced, and therefore, it is very probable that the monolayer starts buckling from the critical pressure, signaling the commencement of nucleation into multilayers in the plateau region of the collapse isotherm. But whereas in StA this nucleation is accompanied with a drop in the surface pressure (signifying loss of material from the monolayer to the aqueous subphase), in FeSt2 this transition takes place on the water surface with a continuous gain in concentration.

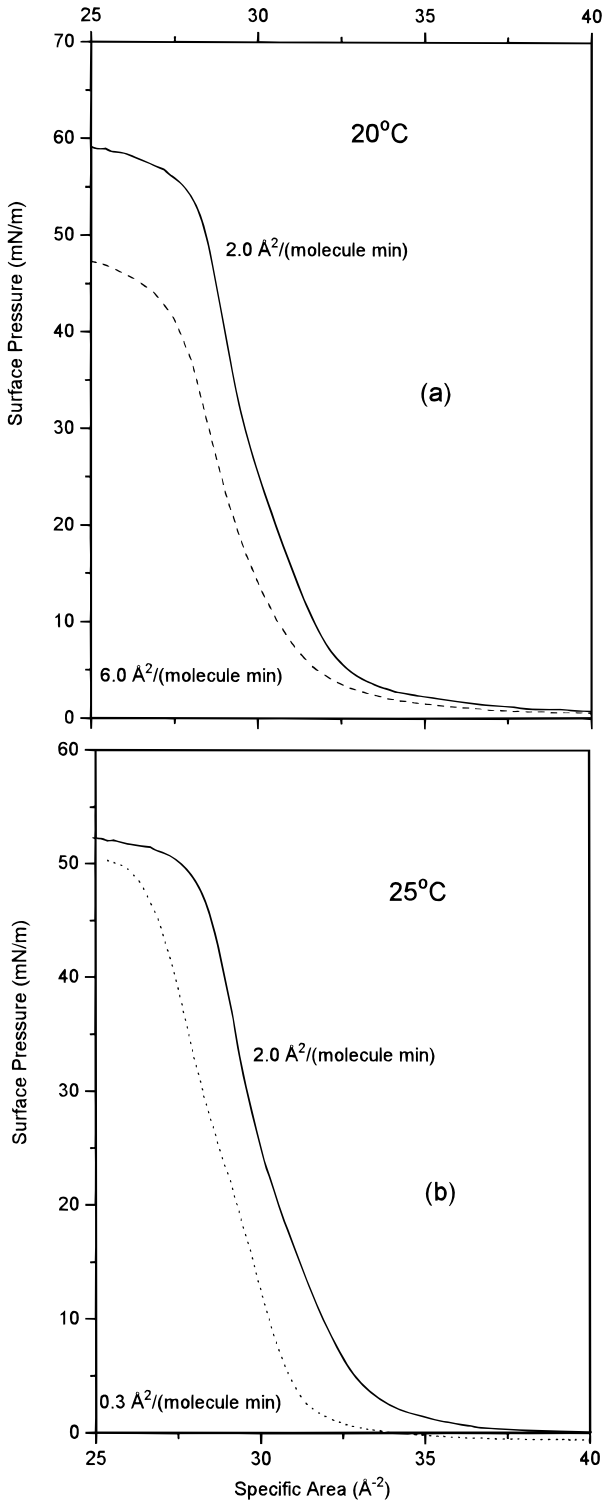


**Figure 4.** Variation of the FeSt2 monolayer on water with compression rate: (a) collapse isotherms at 2.0 (solid line) and 6.0 Å$^2$/(molecule min) (dashed line) compression rates; (b) collapse isotherms at 2.0 (solid line) and 0.3 Å$^2$/(molecule min) (dashed line) compression rates.

## 5. Variations in the Monolayers

**5.1. Variations with Compression Rate and Temperature.** For the larger compression rates of 2.0 and 6.0 Å$^2$/(moleucle min) at 20.0 °C and pH = 5.65 (Figure 4), we find that the collapse pressure of the FeSt2 monolayer reduces with increase in the compression rate. However, a more systematic variation is observed with temperature. This is shown in Figure 5 which shows the COI's for 20, 25, and 30 °C at the same compression rate (2.0 Å$^2$/(molecule min)) and at pH = 5.65. With increase in temperature from 20 to 30 °C there is a definite shift toward

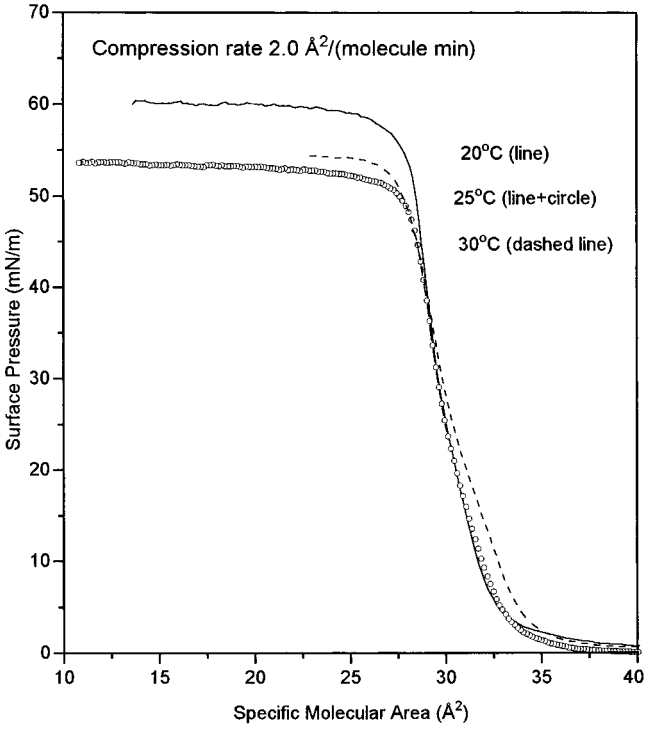


**Figure 5.** Variation of the FeSt2 monolayer on water with temperature. Collapse isotherms at 20 (solid line), 25 (line + circle), and 30 °C (dashed line).

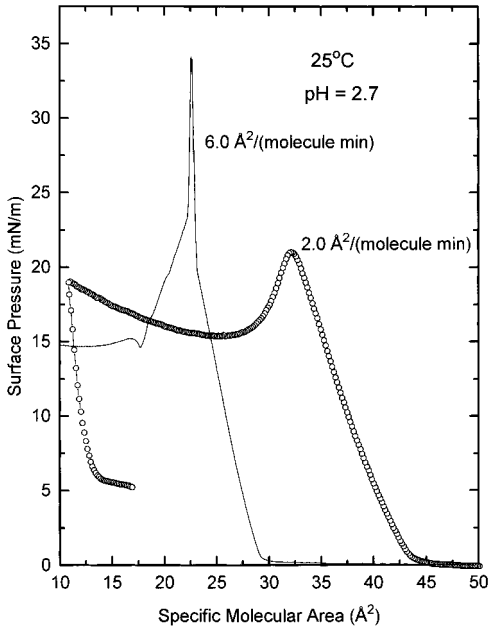


**Figure 6.** Collapse isotherms of stearic acid Langmuir monolayer (line) and FeSt2 monolayer on water (circle) at low pH (∼2.7).

larger areas per molecule, and the "phase- transition kink" at around $\pi = 20$ mN/m, not noticeable at 20 °C, becomes clearly visible. To understand whether this signifies formation of more StA with temperature, we have studied the FeSt2 isotherm at low pH and compared that data with the corresponding data for the StA monolayer and the data on FeSt2 monolayer at corresponding compression rate but at normal pH.

**5.2. Variations with pH.** In Figure 6, the COI's of FeSt2 and StA at 25 °C, compression rates of 2.0 Å²/(molecule min) and 0.6 Å²/(molecule min), and at pH values of 2.73 and 2.75, respectively, are presented. At this low pH, the FeSt2 monolayer collapses similarly as the StA monolayer, but at a very low surface pressure of about 21.0 mN/m and an area per molecule of about 32 Å², which corresponds to a "zero-pressure"

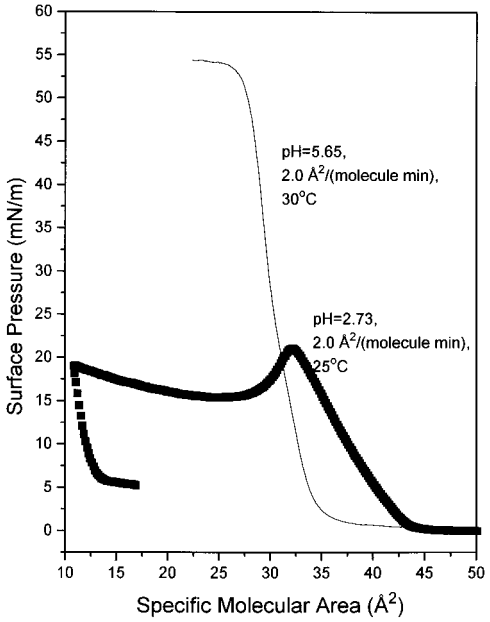


**Figure 7.** Collapse isotherms of FeSt2 monolayer on water at normal (line) and low (square) pH, ∼5.6 and ∼2.7, respectively.

specific molecular area of 42.8 Å². This shows the conversion of the ferric stearate to stearic acid in the monolayer. The low collapse pressure for the FeSt2 monolayer, compared to that of StA (≃34.0 mN/m), indicates that this mixed monolayer is more hydrophilic than the acid monolayer at the same pH. Phases of the monolayer become more well-defined if we plot the isothermal surface compressibility defined as

$$\kappa = -\frac{1}{A}\left(\frac{\partial A}{\partial \pi}\right)_T \qquad (1)$$

as a function of $A$. The COI's of the FeSt2 monolayers at 30 °C and pH = 5.65 and at 25 °C and pH = 2.73 are shown in Figure 7 while the corresponding compressibility versus surface pressure curves are shown in Figure 8, a and b, respectively. The values of surface pressure and area per molecule at collapse for the monolayer at the higher pH are about 52.9 mN/m and 26.8 Å². The "kink" is shown more clearly in Figure 8a as a compressibility maximum (0.005 m/mN) near 20.9 mN/m, almost exactly at the position of the compressibility maximum (1.862 m/mN) at collapse for the monolayer at low pH (Figure 8b). These and the data from FeSt1 (presented in Figure 2b) lead us to correlate the "kink" with presence of free stearic acid in the monolayer.

**5.3. A Model for the FeSt Monolayer.** We have tried to reconcile the experimental findings described above with a simple model of a densely packed monolayer of amphiphile molecules with the headgroups in water and tails perpendicular to the water surface. The headgroup is approximated by a small sphere connected by three equivalent bonds to the hydrocarbon tails, which are approximated by cylinders with an area of 18 Å² each. This model gives a specific molecular area of 44.66 Å². If we invoke a floating bilayer, the specific molecular area for this model would be 22.33 Å².

As both these values are far from the best estimated experimental value of 31.4 Å² we have to discard the conventional structure for a Langmuir film (hydrophilic group in water, hydrophobic group in air) and look for other probable models for the ferric stearate monolayer. In that we are guided by the highly hydrophobic nature of the monolayer, which indicates a structure without appreciable hydrophilic interaction with the aqueous substrate. Experimental evidence of monolayers on water surface formed through van der Waals attractive forces

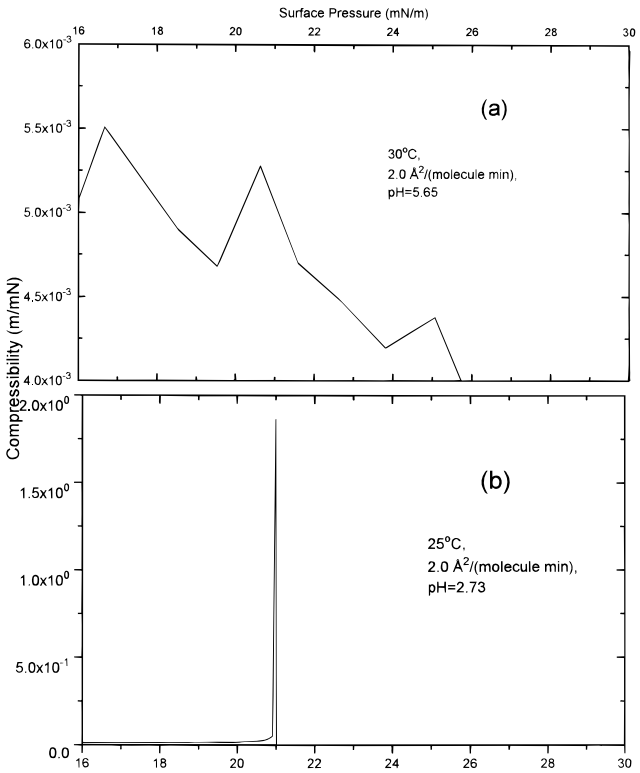


**Figure 8.** Compressibility versus surface pressure curves for FeSt2 monolayers on water at (a) normal pH (∼5.6) and (b) low pH (∼2.7). Refer to text for details.

between long chains and between one end of the chains and the water surface are known for, e.g., perfluoro-*n*-eicosane.[39] In these monolayers the chains are aligned vertically by the hydrophobic repulsion from water. We propose a similar structure for the ferric stearate monolayer.

In our proposed model we retain the simplified cylinder-and-sphere picture for the molecules (with area per cylinder = 18 Å$^2$). However, instead of the headgroup immersed in water, we have one (or two) tails of alternate molecules in contact with the air−water interface, and correspondingly, there is a layer of two (or one) tails of alternate molecules at the top of the film. The headgroups rest between these "tail-layers", each held by the three equivalent bonds to its three tails. From this model the specific molecular area for the monolayer is estimated to be 34.38 Å$^2$, quite close to the experimental value.

It should be noted that in our proposed model the net dipole moment of each molecule is zero, which is a requisite for the monolayer to be stabilized by van der Waals interactions alone. It is also interesting to note that in ferric hydroxy stearate, where one hydrocarbon tail is replaced by a hydroxy group and the molecule has a finite dipole moment located in the Fe(OH)-$(COO)_2$ group, the specific molecular area of the monolayer is 50.4 Å$^2$ in the most condensed phase.[40] This corresponds to the usual structure for an amphiphilic monolayer (allowing for dimerization through oxygen bridges).

When the salt monolayer has free acid as an impurity (Figure 2b), its specific molecular area is reduced in consequence to the lower area occupied by the acid molecules. However, this does not change the hydrophobic nature of the monolayer as there is no change in composition in the salt molecules. On the other hand, decomposition of the salt not only releases free acid, but various hydroxy stearates and other compounds are formed as can be seen by the increased hydrophilic nature and collapse behavior of the resulting mixed monolayer (Figures 6 and 7). We feel that the presence of the hydroxy stearates is responsible for an increase in the specific molecular area at low

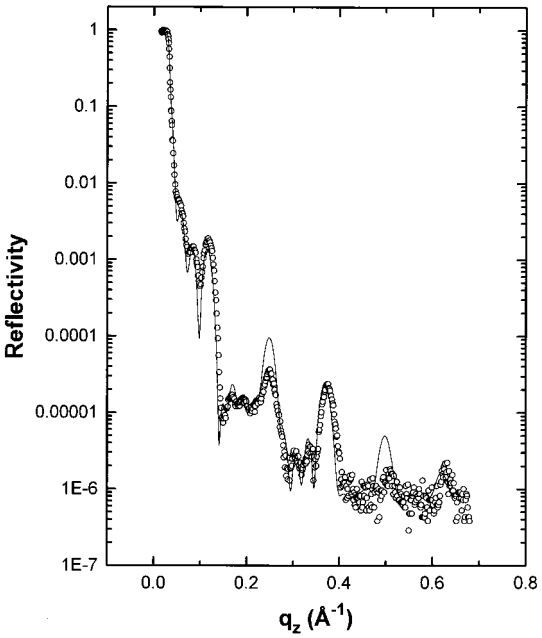


**Figure 9.** X-ray reflectivity profile of the 9-monolayer Langmuir−Blodgett film of FeSt2 on Silicon (100). Experimental data are shown in open circles while the continuous curve represents the profile calculated from the proposed model. Refer to text for details.

pH, which is (42.8 Å$^2$) between that at normal pH (31.14 Å$^2$) and the reported value for ferric hydroxy stearate (50.4 Å$^2$). We also note that there is a drop in the collapse pressure (and hence in the hydrophobicity) with increase in temperature, but as there is lack of consistency in these data, it is difficult to draw any conclusion.

X-ray scattering studies of these monolayer phases are required to understand the structure in detail. We plan to perform these studies in the future. However, to verify our proposed model, we have transferred the monolayers on silicon substrate to study the electron density profile.

### 6. LB Film of Ferric Stearate

In Figure 9 we show the X-ray reflectivity data of the LB film of FeSt2 on Si (open circles). This film has been deposited in nine strokes (five upstrokes and four downstrokes or dips) at $\pi = 30$ mN/m, 25 °C and pH = 5.65. A preliminary analysis of the reflectivity data has been carried out using the Parratt scheme.[41,42] The calculated reflectivity profile is shown in Figure 9 (in line).

We have calculated the reflectivity for the LB film based on our model for the monolayer at the air−water interface. The model used for this calculation assumes a film of four and half bilayers. It starts from the Si substrate with an average electron density (AED) of 0.723*e*/Å$^3$ and absorption coefficient $\mu = 1.4304 \times 10^{-6}$/Å. On this is the first monolayer of the LB film, beginning with its head layer. The four bilayers of the LB film sit on this. Each bilayer has a layer of heads in the middle, one tail layer above it, and one tail layer below it. Our model of the LB film closely follows that proposed by Malik et al.[43] for divalent metal salts of fatty acids. The head/tail ratio is taken to be 1:3, and the area per hydrocarbon chain is taken as 18.0 Å$^2$.[33,34] The length of the tail is half of the bilayer separation which, given by the position of Bragg peaks in Figure 9, is 22.369 Å. The area per head is 31.14 Å$^2$, the observed "zero pressure" area for the densest phase of FeSt2 monolayers. The relevant bond lengths were obtained from standard reference.[44]

The qualitative agreement between the observed and calculated reflectivity, especially for the odd order Bragg peaks and

the Kiessig fringes, as evidenced in Figure 9 provides preliminary justification for our proposed model. Here we assume that a monolayer is transferred on the film with each stroke. On the other hand, a model based on bilayer transfer with each stroke did not at all agree with the data, especially in determining the Kiessig fringes. This indicates that, if we disregard any major structural rearrangement (breakdown of the film on water surface and reconstituition on Si surface, etc.) during transfer, our proposed model for the FeSt2 monolayers on water surface is justified.

## 7. Discussions and Conclusion

We have studied the $\pi-A$ isotherms of Langmuir monolayers of preformed ferric stearate on pure water at different temperatures and compression rates and also on water at a low pH. We have compared these with isotherms of stearic acid on water at normal and low pH and with isotherms of a ferric stearate sample with more stearic acid impurity. We have ascertained the compositions of the two ferric stearate samples in bulk and the composition of a Langmuir−Blodgett film (11 monolayers) of the purified stearate sample (on $CaF_2$ by Fourier transform infrared spectroscopy). An LB film (9 monolayers) of the purified sample on Si have been studied by grazing incidence X-ray reflectivity.

The data from these experiments indicate that ferric stearate on pure water forms a monolayer of molecules with three hydrocarbon tails and an anomalously low specific molecular area, which is very hydrophobic and shows collapse with constant surface pressure under high compression. There is some dissociation with temperature and large dissociation with lowering of pH. The monolayer becomes more hydrophilic by a drop in the pH. We have proposed a model for this monolayer whose interaction with water is predominantly hydrophobic with one (or two) tails of alternate molecules in contact with the air−water interface. It has a head/tail ratio of 1:3 and a specific molecular area of 18 $Å^2$. This model gives a specific molecular area that is close to the observed value and a plausible explanation of the results of experiments on the monolayer. The model was used to calculate the X-ray reflectivity of the 9-monolayer LB film of FeSt on Si, and the calculated values are qualitatively consistent with the corresponding experimental values. The decompression curve for this monolayer is, in general, very different from the compression curve and starts with a sharp drop in surface pressure with almost no change in specific molecular area. It has been reported that at low surface pressures a fatty acid Langmuir monolayer breaks up into islands of close packed molecules that are perpendicular to the surface at pH $\simeq$6.0.[14] We believe that during decompression from a condensed phase the ferric stearate monolayer undergoes a similar fragmentation into large islands within which the specific molecular area remains almost unchanged from that just before decompression, while the surface pressure is drastically reduced due to the penetration of water between the islands. Below a certain surface pressure ($\simeq$22.0 mN/m) the islands start breaking down continuously to finally enter the dilute phase.

**Acknowledgment.** We express our sincere gratitude to Prof. J. Dutta, Institute of Wetland Management and Ecological Design, for his help and advice in the preparation and initial purification of the ferric stearate sample. We thank Prof. S. S. Talwar, Chemistry Department, Indian Institute of Technology, Mumbai, and Prof. N. Chatterjee, Condensed Matter Physics Group, Saha Institute of Nuclear Physics, for many useful discussions and suggestions.

## References and Notes

(1) Langmuir, I. *J. Am. Chem. Soc*. **1917**, *39*, 1848.

(2) Langmuir, I. *Trans. Faraday Soc*. **1920**, *15*, 62. Blodgett, K. B. *J. Am. Chem. Soc*. **1935**, *57*, 1007.

(3) Harkins, W. E.; Copeland, L. E. *J. Chem. Phys*. **1942**, *10*, 272. Kaganer, V. M.; Loginov, E. B. *Phys. Rev. Lett*. **1993**, *71*, 2599.

(4) Kjaer, K.; Als-Nielsen, J.; Helm, C. A.; Laxhuber, L. A.; Möhwald, H. *Phys. Rev. Lett*. **1987**, *58*, 2224.

(5) Knobler, C. M. *Adv. Chem. Phys*. **1990**, *77*, 397.

(6) Dutta, P. In *Phase Transitions in Surface Films 2*; Taub, H., et al., Eds.; Plenum Press: New York, 1991.

(7) Kenn, R. M.; Böhm, C.; Bibo, A. M.; Peterson, I. R.; Möhwald, H.; Als-Nielsen, J.; Kjaer, K. *J. Phys. Chem*. **1991**, *95*, 2092.

(8) Bohanon, T. M.; Lee, A. M.; Ketterson, J. B.; Dutta, P. *Langmuir* **1992**, *8*, 2497.

(9) Möhwald, H. *Rep. Prog. Phys*. **1993**, *56*, 653.

(10) Als-Nielsen, J.; Jacquemain, D.; Kjaer, K.; Leveiller, F.; Lahav, M.; Leiserowitz, L. *Phys. Rep*. **1994**, *246*, 251.

(11) Kaganer, V. M.; Peterson, I. R.; Kenn, R. M.; Shih, M. C.; Durbin, M.; Dutta, P. *J. Chem. Phys*. **1995**, *102*, 9412.

(12) Bommarito, G. M.; Foster, W. J.; Pershan, P. S.; Schlossman, M. L. *J. Chem. Phys*. **1996**, *105*, 5265.

(13) Dutta, P.; Peng, J. B.; Lin, B.; Ketterson, J. B.; Prakash, M.; Georgopoulos, P.; Ehrlich, S. *Phys. Rev. Lett*. **1987**, *58*, 2228.

(14) Grundy, M. J.; Richardson, R. M.; Roser, S. J.; Penfold, J.; Ward, R. C. *Thin Solid Films* **1988**, *159*, 43.

(15) Lin, B.; Peng, J. B.; Ketterson, J. B.; Dutta, P. *Thin Solid Films* **1988**, *159*, 111.

(16) Leveiller, F.; Jacquemain, D.; Lahav, M.; Leiserowitz, L.; Deutsch, M.; Kjaer, K.; Als-Nielsen, J. *Science* **1991**, *252*, 1532.

(17) Shih, M. C.; Bohanan, T. M.; Mikrut, J. M.; Zschack, P.; Dutta, P. *J. Chem. Phys*. **1992**, *96*, 1556.

(18) Böhm, C.; Leveiller, F.; Jacquemain, D.; Möhwald, H.; Kjaer, K.; Als-Nielsen, J.; Weissbuch, I.; Leiserowitz, L. *Langmuir* **1994**, *10*, 830.

(19) Leveiller, F.; Böhm, C.; Jacquemain, D.; Möhwald, H.; Leiserowitz, L.; Kjaer, K.; Als-Nielsen, J. *Langmuir* **1994**, *10*, 819.

(20) Prakash, M.; Dutta, P.; Ketterson, J. B.; Abraham, B. M. *Chem. Phys. Lett*. **1984**, *111*, 395.

(21) Jark, W.; Comelli, G.; Russell, T. P.; Stöhr, J. *Thin Solid Films* **1989**, *170*, 309.

(22) Sanyal, M. K.; Sinha, S. K.; Gibaud, A.; Huang, K. G.; Carvalho, B. L.; Rafailovich, M.; Sokolov, J.; Zhao, X.; Zhao, W. *Europhys. Lett*. **1993**, *21*, 691.

(23) Schwartz, D. K.; Viswanathan, R.; Garnaes, J.; Zasadzinski, J. A. *J. Am. Chem. Soc*. **1993**, *115*, 7374.

(24) Viswanathan, R.; Zasadzinski, J. A.; Schwartz, D. K. *Science* **1993**, *261*, 449.

(25) Zasadzinski, J. A.; Viswanathan, R.; Madsen, L.; Granaes, J.; Schwartz, D. K. *Science* **1994**, *263*, 1726.

(26) Schwartz, D. K.; Viswanathan, R.; Zasadzinski, J. A. *J. Chem. Phys*. **1994**, *101*, 7161.

(27) Prakash, M.; Peng, J. B.; Ketterson, J. B.; Dutta, P. *Thin Solid Films* **1987**, *146*, L15.

(28) Giesse, E.; Deugler, J.; Ritter, G.; Wagner, W.; Brandl, D.; Voit, H.; Saemann-Ischenko, G. *Solid State Commun*. **1993**, *86*, 243.

(29) Faldum, T.; Meisel, W.; Gütlich, P. *Hyperfine Interact*. **1994**, *92*, 1263. Faldum, T.; Meisel, W.; Gütlich, P. *Appl. Phys. A* **1996**, *62*, 317.

(30) Giesse, E.; Ritter, G.; Brandl, D.; Voit, H.; Rozlsonik, N. *Hyperfine Interact*. **1995**, *95*, 175.

(31) Marshbanks, T. L.; Franses, E. L. *J. Phys. Chem*. **1994**, *98*, 2166.

(32) Gaines, G. L. *Insoluble Monolayers at the Liquid−Gas Interface*; Interscience: New York, 1966.

(33) Kitaigorodskii, A. I. *Organic Chemical Crystallography*; Consultant Bureau: New York, 1961.

(34) Bonnerot, A.; Chollet, P. A.; Frisby, H.; Hoclet, M. *J. Chem. Phys*. **1985**, *87*, 365.

(35) Siegel, S.; Hönig, D.; Vollhardt, D.; Möbius, D. *J. Phys. Chem*. **1992**, *96*, 8157.

(36) McFate, C.; Ward, D.; Olmstead III, J. *Langmuir* **1993**, *9*, 1036.

(37) Birdi, K. S.; Vu, D. T. *Langmuir* **1994**, *10*, 623.

(38) Hu, J.-G.; Granek, R. *J. Phys. II (Paris)* **1996**, *6*, 999.

(39) Li, M.; Acero, A. A.; Huang, Z.; Rice, S. A. *Nature* **1994**, *367*, 151.

(40) Kongzhang, Y.; Jin, M.; Xusheng, F.; Jingen, C. *Thin Solid Films* **1989**, *178*, 341.

(41) Parratt, L. G. *Phys. Rev*. **1954**, *95*, 359.

(42) Sanyal, M. K.; Datta, A.; Banerjee, S.; Srivastava, A. K.; Arora, B. M.; Kanakaraju, S.; Mohan, S. *J. Synchrotron Radiat*. **1997**, *4*, 185.

(43) Malik, A.; Durbin, M. K.; Richter, A. G.; Huang, K. G.; Dutta, P. *Phys. Rev. B* **1995**, *52*, R11654.

(44) Pauling, L. *The Nature of the Chemical Bond*; Cornell University Press: Ithaca, NY, 1960.